RSC Advances

ROYAL SOCIETY OF CHEMISTRY

www.rsc.org/advances

Sorption and photodegradation of tylosin and sulfamethazine by humic acid-coated goethite

Xuetao Guo[1], Jing Zhang[1], Jianhua Ge[1], Chen Yang[2*], Zhi Dang[2], Shaomin Liu[1], Liangmin Gao[1]

[1] *School of Earth and Environment, Anhui University of Science and Technology, Huainan 232001, China*

[2] *College of Environment and Energy, South China University of Technology, Guangzhou, 510006, China*

*Corresponding authors: Tel: +86-20-87110198, Fax: +86-20-39380508;

E-mail addresses: cyanggz@scut.edu.cn (C. Yang).

Abstract

Humic acid and mineral oxides were simultaneously present in soils and could form organomineral complexes. These complexes could influence the transport and fate of antibiotics in the environment. The objective of this study was to investigate the sorption and photodegradation of TYL and SMT on these complexes. The results showed HA tended to interact with goethite via hydrophobic and π-π interactions. The sorption capacity and sorption rate gradually increased with the concentrations of HA increased and the equilibrium time for TYL and SMT were 7 h and 24h respectively on HA -goethite complexes. The sorption isotherms of TYL were more nonlinear and SMT were less nonlinear on HA-goethite complexes with the concentrations of HA increased, which implyed a more heterogeneous distribution of the sorption sites for TYL and more rigid and porous structures were developed for SMT. The photodegradation of TYL and SMT by HA-goethite complexes were increased with the concentrations of HA increased. An iron redox cycle coupled should be a common phenomenon in the system, since both Fe(III) and HA were ubiquitous in the natural environment. It should be noticed the influence of HA and goethite on the fate of antibiotics in the environment. This study is helpful in understanding the potential of toxic organic pollutants migration and transformation in natural environmental.

Keywords: sorption, photodegradation, antibiotics, HA-goethite complexes

1. Introduction

Tylosin (TYL) and sulfamethazine (SMT) were widely used in aquiculture and livestock industry as the typical antibiotic and had drawn growing attention. They entered into the environmental

matrices by direct runoff and excretion as unmetabolized drugs or active metabolites and degradation products [1]. Recently, it has been reported that TYL and SMT were detected in surface water, wastewater and soils [2]. The occurrence of cumulated TYL and SMT in the environment could induce genetic exchange, increase the resistance of bacteria against drugs and subsequently threaten human health [3, 4]. Sorption and degradation were important processes that controlled the transport, fate, bioavailability and ecotoxicological risk of TYL and SMT in the environment, thus a through understanding of sorption and degradation were the central importance for predicting mobility and availability of TYL and SMT in soils [5].

Although many experiments have focused on the sorption of TYL and SMT onto soils or soil components, the full mechanism of sorption was still not completely clearly[1, 6, 7]. Humic substances bound strongly to metal oxide and hydroxide particles, and such associations occurred in the solid phase of soils and sediments [8]. It was well known that ion binding to oxides was somewhat dependent on the electrostatic potential profile in the vicinity of the surface and this potential profile would be strongly affected by the presence of adsorbed humic substances [9]. Goethite (α-FeOOH) is one of the most common and stable crystalline iron oxide in sediments and natural systems [10]. This mineral has a relative high surface area and high reactivity which could be suitable for sorption and deactivation of pesticides, nutrients, and hazardous compounds in natural conditions, and might greatly affect the distribution and transport of contaminants in the environment [7]. Previous studies have shown that sorption of TYL and SMT on goethite was strongly dependent on pH and ionic strength, and has been suggested to be due to the favourable interaction between TYL/SMT and the positively charged surface of the iron oxides [3, 7, 11, 12]. Goethite was also found associated with organic matter in soils. This mutual interaction could modify the individual reactivity of both organic

matter and the mineral surface affecting the cycle of the various chemical species present in soil [11]. Some researchers suggested that coated HA could significantly promoted sulfonamide sorption in comparison to mineral particles which was explained by the specific interactions between sulfonamide and organic functional groups [13].

Except for the sorption of contaminants, goethite also decomposes or catalyze the decomposition of some contaminants in the absence and presence of hydrogen peroxide and/or UV radiation [14, 15]. Recently, Han et al. first reported that aqueous goethite can generate singlet oxygen and hydroxyl radical under room light and aeration conditions investigated using spin trapping electron paramagnetic resonance and H_2O_2 can improve the generation of both reactive species [14]. The similar result could be found in the report indicating goethite surfaces catalysed a Fenton-like reaction responsible for the decolorizing of azo dye Orange G [15]. However, the treatment of antibiotic by goethite has not been documented, and little information has been obtained about the transform of antibiotic in the natural environment system.

In this paper, our aims were to investigate TYL and SMT sorption and degradation by organo-goethite complexes and the possible effect of sorption parameters on its degradation. For this purpose, our study was conducted in three parts: 1) the use of goethite and well-characterized organo-goethite complexes should provide better understanding of mechanisms controlling TYL and SMT sorption and their influence on its degradation. 2) the sorption of TYL and SMT by goethite with their complexes with different concentrations of HA; 3) the degradation of TYL and SMT in the presence of goethite with their complexes with different concentrations of HA.

2. Materials and methods

2.1. Materials and preparation

Tylosin tartrate (purity>95%) and sulfamethazine (purity>99%) were purchased from Sigma-Aldrich Corporation (St Louis, MO). Acetonitrile and formic acid (HPLC grade, Merck Chemicals Co. AQ5) were used as received. Pure water was prepared by Milli-Q® water machine (Millipore Co., Guangzhou, China). All the other chemicals were analytical reagent grade and used without further purification.

TYL and SMT, like most antibiotics, are ionic compounds. TYL is a weak base with a pK_a of 7.1. In acidic conditions, there might be formed ionic bonds between protonated TYL and anionic components of soil and manure matrices. SMT is an amphoteric compound with pK_a values at 2.28 and 7.42 respectively. The net charges of SMT in different pH conditions would be more complicated and lead to heterogeneous sorption activities between SMT and solid phase.

Humic acids (solid granule, particle size is 0.4-0.6 μm) used throughout this investigation was obtained from JuFeng Chemical Corporation, Shanghai, China. The elemental composition of HA is: 52.37% C, 3.57% H, 36.12% O, and 1.80% N.

Primary stock solutions of TYL and SMT at 1,000 mg/L were prepared with pure water and stored at 4 ^{o}C for a maximum of 1 month. The work solutions were prepared by diluting stock solution using 0.01 M KNO_3 solution.

2.2. Preparation and characterization of goethite and HA-goethite complexes

Goethite was synthesized according to the method introduced by Brigante et al [16]. In brief, 5 M KOH was added into 0.5M $Fe(NO_3)_3$ until red colloid was generated. The resulting ferrihydrite dispersion was aged at 60 ^{o}C in a capped Teflon container during 60 h and then it was washed with

double distilled deionized (DDI) water until the supernatant reached a pH close to the point of zero charge. After that, the dispersion was freeze-dried in order to obtain a dry powder.

The HA–goethite complexs were synthesized according to Yang and Xing [17] with minor modification. Briefly, 5 g goethite and was mixed with 1 L HA solution in a bottle and shaken for 2 days, after which the suspensions were centrifuged at 3500 g for 30 min. The precipitated materials were freeze-dried, ground, and stored for future experiments. HA solution was obtained by dissolving solid HA with 0.1 M NaOH, and adjusting to pH 5. HA concentrations in solution were 50, 100, 200, and 500 mg/L.

The general characterization of the synthesized goethite and HA-goethite complexes were performed by X-ray diffraction (XRD), FT-IR, SEM, Raman spectroscopy and the N_2-BET. XRD patterns were obtained using a Bruker D8 X-ray diffractometer with Cu-Ka Xray source (λ =0.15418 nm). FT-IR spectra were obtained with a Nicolet FT-IR Nexus 470 Spectrophotometer. The samples were dried under vacuum until constant weight was achieved and diluted with KBr powder (1%) before the FT-IR spectra were recorded. The morphologies were recorded with a scanning electron microscope (SEM, JEOL JSM-6510LV), which was operated at an acceleration voltage of 10 kV. Raman spectroscopy (Jobin Yvon T64000) was used to further characterize goethite and HA-goethite complexes. The N_2-BET adsorption at 77K was measured with a Quantachrome Nova 1200e instrument. Each sample was degassed under vacuum at 30 ^{o}C for 60 min prior to analysis. The point of zero charge (PZC) of goethite was measured by potentiometric titrations at three KCl concentrations.

2.3. Sorption procedure

The sorption experiments were conducted using a batch equilibrium technique. TYL and SMT were mixed at high concentration in methanol before being added to background solution. The background solution contained 0.003 M NaN_3 to minimize bioactivity and 0.01 M KNO_3 to adjust ionic strength. A predetermined amount of goethite and HA-goethite complexes with filled with the initial aqueous solution in completely mixed batch reactor (CMBR) systems with teflon gaskets and mixed for sorption equilibrium on a shaker at 150 rpm. After sorption experiments, the screw cap vial were centrifuged at 4000 rpm for 30 min, and 1 mL of supernatant was transferred to a pre-weight 1.5 mL amber glass vial for chemical analyses. Each concentration level, including blanks, was run in three parallels. KOH or HNO_3 solutions were used for pH adjustment.

Kinetic studies of TYL and SMT sorption on goethite and HA-goethite complexes were carried out from aqueous solutions with a certain concentration and pH. A fixed volume of the aliquot was withdrawn at designated time points while the reactors were run continuously. In order to investigate the influences of temperature, the shaker was adjusted at the desired temperature.

2.4. Sorption models

The equilibrium sorption data was fitted using Henry (Equation 1), Langmuir (Equation 2) and Freundlich (Equation 3) models [18]:

$$q_e = k_d c_e \qquad (1)$$

$$q_e = \frac{q_m b C_e}{1 + b C_e} \qquad (2)$$

$$q_e = k_f C_e^{\,n} \qquad (3)$$

Where C_e (mg/L) and q_e (mg/kg) are the equilibrium concentration of TYL and SMT in the liquid phase and solid phase, respectively; k_d (L/kg) is the distribution coefficient of solute between soil and water. The b and q_m are the Langmuir constants, which are related to the sorption bonding energy and

the maximum sorption capacity; k_f (μg/g)/(mg/L) is the capacity affinity parameter and n (dimensionless) is the exponential parameter. Parameters were estimated by nonlinear regression weighted by the dependent variable.

To investigate the potential rate-controlling steps involved in the sorption of TYL and SMT on goethite and HA-goethite complexes, pseudo-first-order model and pseudo-second-order kinetic model were employed to fit the data [7].

The pseudo-first-order rate expression is generally expressed as follows:

$$\frac{\mathrm{d}q_e}{\mathrm{d}t} = k_1(q_e - q_t) \quad (4)$$

After integration with the initial condition $q_t = 0$ at $t = 0$, Eq. 4 can be obtained.

$$\log(q_e - q_t) = \log q_e - \frac{k_1 t}{2.303} \quad (5)$$

The pseudo-second-order mpdel is given as:

$$\frac{t}{q_t} = \frac{1}{k_2 q_e^2} + \frac{t}{q_e} \quad (6)$$

Where q_e and q_t were the amounts of sorption TYL and SMT at equilibrium and time t respectively. k_1 (h^{-1}) and k_2 (g/μg/h) are the sorption rate constant of pseudo-first-order and pseudo-second-order sorption rate, respectively. The rate constants k_1 and k_2 can be derived from linear regressions based on experiment results.

2.5. Photodegradation study.

The photodegradation experiments of were performed in a slurry reactor containing a solution of TYL and SMT (200 mL, 10 mg L^{-1}) and the goethite and HA-goethite complexes. A Xe lamp was used as a sunlight source. Prior to irradiation, the suspension was kept in the dark under strong magnetic stirring for 12 h to ensure the establishment of an sorption/desorption equilibrium. At given

time intervals, aliquots of about 2 mL were collected from the suspension and centrifuged immediately and then 1 mL of supernatant was transferred to a pre-weight 1.5 mL amber glass vial for chemical analyses.

2.6. Chemical Analysis

The concentrations of TYL and SMT in aqueous solution were measured by a reverse-phase high-performance liquid chromatography (Agilent 1200) with C_{18} column (5 μm, 4.6×250 mm; Agilent) and diode array UV detector (wavelength at 290 nm for TYL and 264 nm for SMT). The mobile phase (at a flow rate of 0.5 mL/min) for TYL was a mixture of acetonitrile (35%) and an aqueous solution (65%) containing 0.01 mol/L KH_2PO_4 (pH = 2.0) but for SMT it was a mixture of acetonitrile and formic acid solution (0.05% v/v) at a volumetric ratio of 60:40 with a flow rate of 1 mL/min . The injection volume was 20 μL. External standards of TYL and SMT (0.1-100 mg/L) were employed to establish a linear calibration curve and the sample concentrations were calculated from its integrated peak areas. The solid phase concentrations were calculated based on the mass balance of the solute between the two phases. Concentration of H_2O_2 was determined using a colorimetric method developed by Ou et al.[19], and concentration of Fe(II) was determined using the ophenanthroline method by a spectrophotometer (Jasco UV-550,Japan).

3. Results and discussion

3.1. Characterization of the goethite and HA-goethite complexes

The goethite and HA-goethite complexes were examined by TEM and SEM at high magnification were shown in Fig. 1. The particles of goethite could be observed like needle shaped with 50-100 nm width and 0.5-1 μm length (Fig. 1a and b). The surface morphology of goethite changed significantly

after HA immobilization. The image of HA-goethite complexes displayed a irregularity surface (Fig. 1c and d). From this image we can say that the HA molecules have been immobilized onto the surface of goethite after the contact of goethite with HA solution. The specific surface area of goethite and HA-goethite complexes were 34.11, 33.28, 35.27, 37.12, 36.78 m^2/g based on N^2-BET sorption with the concentrations of HA were 50ppm, 100ppm, 200ppm and 500ppm.

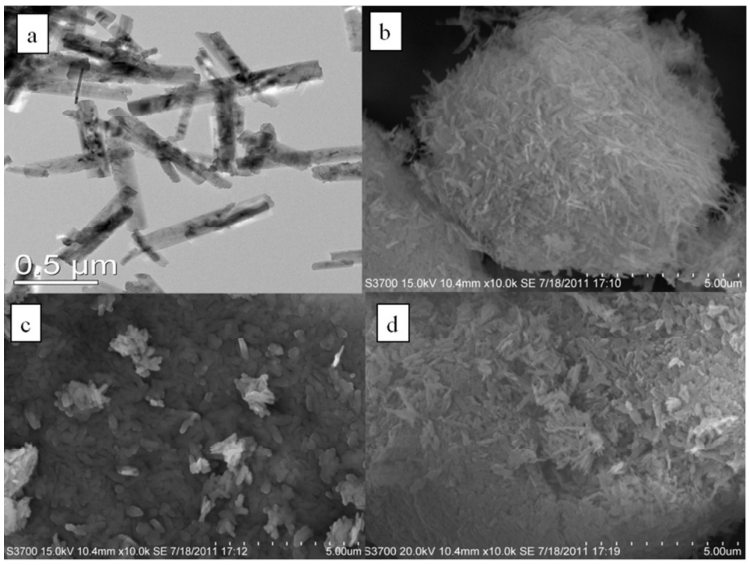

Fig. 1 TEM image of goethite (a), SEM images of goethite (b), 100ppm HA -goethite complexes (c) and 500ppm HA -goethite complexes (d)

The XRD patterns of goethite and HA-goethite complexes were shown in Fig.2. All the peaks in the pattern were labeled and indexed to a tetragonal goethite phase (JCPDS file no. 34-1266), indicating that goethite was synthesized without any detectable impurity [3]. After combining goethite and HA at different concentrations of HA, all the peaks of as-prepared goethite were still observed, implying that HA-goethite complexes were retained in the composition. This result indicated that the crystal structure of goethite was not changed after modification with HA [7, 10, 20].

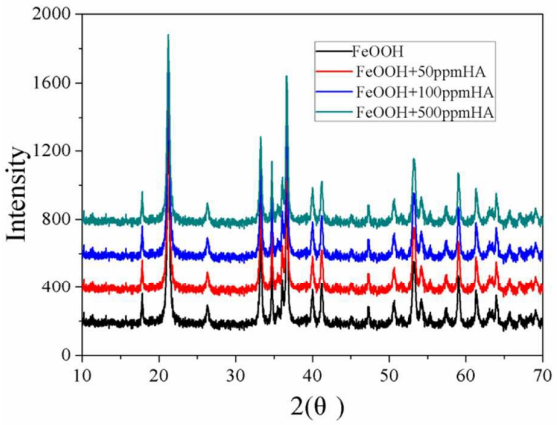

Fig. 2 XRD patterns of goethite and HA -goethite complexes

The surface chemistry of goethite and HA -goethite complexes were studied using FTIR spectrum. Fig. 3 showed the Fe-O stretches of HA -goethite complexes at 1630 cm^{-1}, indicating the hydroxy interacting with the goethite surface[21]. The band at 3400 cm^{-1} corresponding to the OH stretching of the hydroxyl surface groups almost weaken with the concentrations of HA increased [7]. The band at 3125 cm^{-1} possibly corresponded to the bulk OH stretching were stronger with the concentrations of HA increased [3]. The band at 1376 cm^{-1} was most likely due to the $-CH_2$ scissoring. For the bare goethite materials, however, the weakly C=O stretches was observed, and no C-O stretches in found, suggesting the binding of HA to goethite. It is generally believed the binding of HA to goethite surface is mainly through ligand exchange [21, 22].

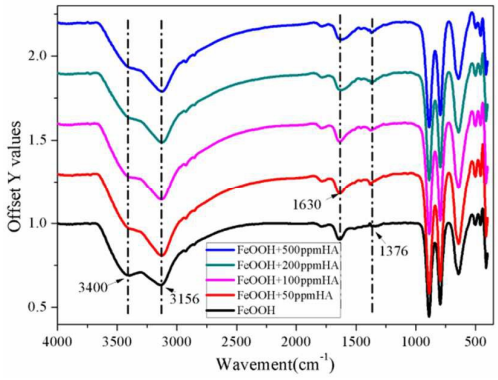

Fig. 3 FTIR spectrum of goethite and HA -goethite complexes

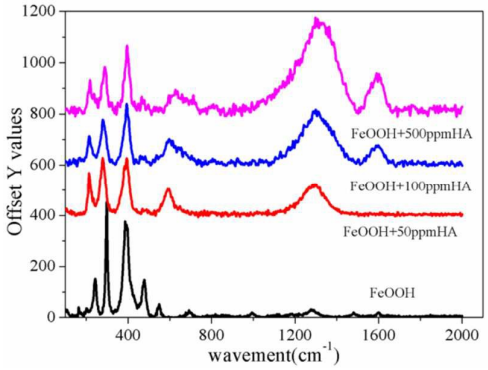

Fig. 4 Raman spectra of goethite and HA -goethite complexes

Further information on the structure of goethite and HA -goethite complexes was obtained using Raman spectroscopy. Each of the spectra shown in Fig. 4 exhibits peaks at 200-500 cm^{-1} and 500-1800 cm^{-1}, which could be assigned to the Raman vibrations of Fe-O and symmetric -OH intermolecular stretching vibration, respectively [23]. These results confirm that the addition of HA has no effects on the crystal structure of goethite, in agreement with XRD analysis. The peaks are observed at around 572, 1257 and 1511 cm^{-1} which were correlation with C=C, Fe-O-C and C=O stretching vibration, which confirmed that the surface structure changes of goethite. The shifts of aromatic C=C and C=O bands were indicative of hydrophobic and π-π interactions between HA and goethite[23].

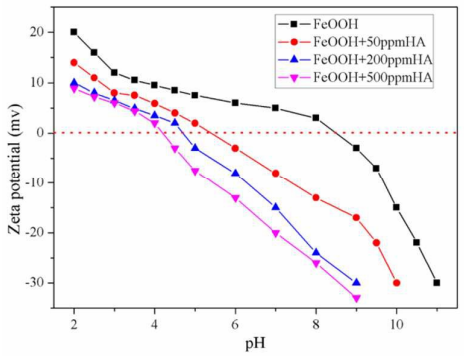

Fig. 5 Zeta potentials of goethite and HA -goethite complexes

The zeta potentials of goethite and HA -goethite complexes were measured at varied pH and shown in Fig. 5. The pH_{PZC} of HA -goethite complexes decreased since the coated HA had abundant

carboxylic acid groups. The zeta potential of gray humic acid is negatively charged in the range of pH 2-11 [21]. The low pH_{PZC} indicated that the HA -goethite complexes were negatively charged at the entire environmentally relevant acidity (pH 3-9), which prohibited the aggregation of HA -goethite complexes and benefited the sorption of positively charged substance.

3.2. Sorption kinetics of TYL and SMT on goethite and HA -goethite complexes

The effect of time for TYL and SMT sorption onto goethite and HA -goethite complexes was illustrated in Fig. 6. It was found that the sorption increased with increasing contact time and nearly 90% of the sorption capacity for TYL and SMT were accomplished within the first 2 h and 7h. Then, the sorption gradually increased at a much slower rate and became almost constant nearly after 7 h and 24 h for TYL and SMT, which represented that the equilibrium time reached.

Table 1 The pseudo-first-order and pseudo-second-order sorption models constants of TYL and SMT on goethite and HA –goethite complexes

Conditions		pseudo-first-order		pseudo-second-order	
		k_1(1/min)	R^2	k_2(g/mg/min)	R^2
TYL	0 ppm HA	0.028	0.753	0.687	0.999
	50 ppm HA	0.058	0.846	1.432	0.999
	100 ppm HA	0.063	0.810	1.501	0.999
	200 ppm HA	0.068	0.894	1.586	0.999
	500 ppm HA	0.073	0.874	1.621	0.999
SMT	0 ppm HA	0.211	0.991	0.258	0.998
	50 ppm HA	0.323	0.973	0.513	0.999
	100 ppm HA	0.376	0,896	0.586	0.999
	200 ppm HA	0.443	0.912	0.632	0.999
	500 ppm HA	0.496	0.908	0.685	0.999

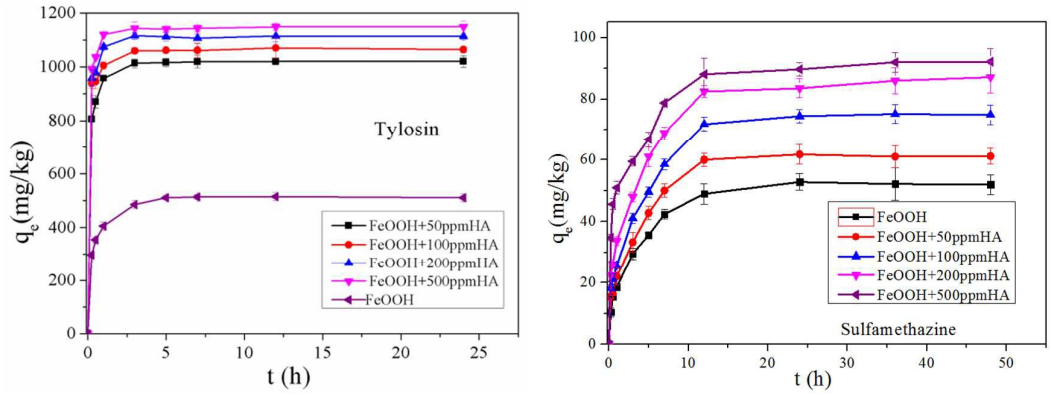

Fig. 6 Sorption kinetics of TYL and SMT on goethite and HA -goethite complexes (equilibrium pH for TYL and SMT were 3.5; temperature = 25 ^{0}C; I = 0.01 M KNO_3)

From the sorption results, two kinetic models were generated to assess the kinetic characteristics of TYL and SMT sorption on goethite and HA-goethite complexes. Table 1 showed the parameters of simulated sorption kinetics models. The results proved that the pseudo-second-order could better explain the sorption processes of TYL and SMT on goethite and HA-goethite complexes with correlation coefficient consistently $R^2 > 0.998$. It was obvious that the sorption rate (k_1 and k_2) for TYL and SMT increased with the concentrations of HA increased and the sorption capacity was also increased with the concentrations of HA increased. The initial sorption rate may be attributed to chemical and/or hydrogen (H) bonding between TYL /SMT and the surface hydroxyls of the goethite [24]. As shown in Table 1, the rate constant (k_2) for TYL was larger than SMT at the same conditions, indicating that the sorption of TYL on goethite and HA-goethite complexes was a faster process and this can be proved by the equilibrium time. This may be due to the difference of sorption force for TYL and SMT [7, 25, 26].

3.3. Sorption isotherms of TYL and SMT on goethite and HA -goethite complexes

Sorption isotherms of TYL and SMT on goethite and HA -goethite complexes were presented in Fig. 7. The sorption data were fitted to the linear, Freundlich and Langmuir isotherms. The sorption data could be fitted well by Freundlich and Langmuir models, as indicated by the high regression coefficient ($R^2 > 0.940$), and the fitting parameters were listed in Table 2.

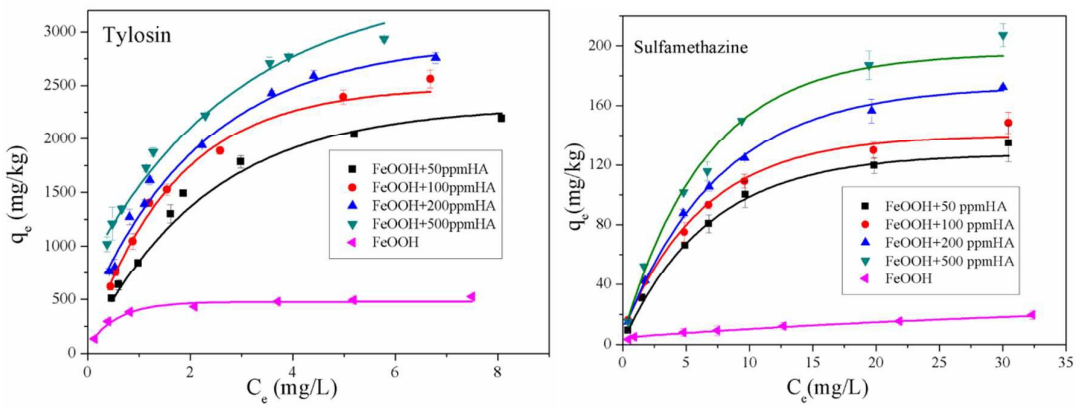

Fig. 7 Sorption isotherms of TYL and SMT on goethite and HA-goethite complexes (equilibrium pH for TYL and SMT were 3.5; temperature = 25 ^{0}C; I = 0.01 M KNO_3; equilibrium time were 24 h)

For original goethite, the isotherms of TYL were more nonlinear as suggested by the low linearity index (n=0.16). As the concentrations of HA increased from 50 ppm to 500 ppm, the n values (0.51-0.67) increased, implying a more heterogeneous distribution of the sorption sites for TYL. In contrast, sorption of SMT on goethite and HA -goethite complexes generally less nonlinear than that of TYL with n values (0.84-0.58) decreased, implying that more rigid and porous structures were developed, which was evidenced by the increased surface C content [27, 28].

TYL and SMT sorption by HA -goethite complexes were higher than goethite (Fig. 7). Li et al. reported that nanoparticle aggregates were dispersed after HA coating [29], and thus the available surface area increased for phenanthrene sorption. According to our measurements of surface areas, goethite aggregate status was not significantly increased after HA coating. Thus the size effect on TYL and SMT sorption could be excluded. Considering the higher sorption of both chemicals on HA than on goethite, the increased sorption of HA -goethite complexes in comparison to goethite particles may be mostly attributed to the adsorbed HA.

TYL and SMT sorption on sorbents is highly affected by their speciation [3]. TYL and SMT have various species in aqueous solution which is dependent on solution pH. In this study, more than 98% of TYL molecules (pK_a=7.1) were positive charged in the test pH (3.5 ± 0.2) which resulted in the electrostatic repulsion decreased with the concentrations of HA increased from 50 ppm to 500 ppm. In comparison, SMT molecule (pK_{a2}=7.23) existed as neutral species at the test pH, and it could be more strongly adsorbed on the hydrophobic carbon surface of HA. Similar results were reported by Peng et al. [25] that nano iron oxides coated HA can increased ofloxacin and norfloxacin sorption.

Table 2 List of TYL and SMT sorption isotherm parameters on goethite and HA-goethite complexes

	Conditions	Henrymodel			Freundlich model		Langmuir model		
		k_d(L/kg)	R^2	n	k_f(μg/g)/(mg/L)^n	R^2	q_e(mg/Kg)	b	R^2
TYL	FeOOH	10.7	0.721	0.16	418	0.959	698	3.38	0.951
	FeOOH+50ppmHA	218.2	0.807	0.51	869	0.946	2034	3.85	0.962
	FeOOH+100ppmHA	272.3	0.829	0.57	992	0.968	2298	4.28	0.971
	FeOOH+200ppmHA	312.3	0.845	0.62	1135	0.984	2435	4.62	0.959
	FeOOH+500ppmHA	372.5	0.884	0.67	1246	0.979	2678	4.89	0.987
SMT	FeOOH	1.02	0.964	0.84	4.87	0.985	19.2	0.12	0.948
	FeOOH+50ppmHA	4.19	0.812	0.71	16.6	0.957	112	0.21	0.945
	FeOOH+100ppmHA	4.68	0.837	0.66	23.2	0.963	127	0.25	0.962
	FeOOH+200ppmHA	5.18	0.894	0.61	28.7	0.978	149	0.36	0.978
	FeOOH+500ppmHA	5.52	0.835	0.58	37.9	0.987	173	0.41	0.949

3.4. Photodegradation of TYL and SMT by goethite and HA -goethite complexes

Fig. 8 showed the photodegradation of TYL and SMT by goethite, HA and HA -goethite complexes at pH 3.5. At the irradiation time of 120 min, the photodegradation of TYL and SMT was observed and the photodegradation rate were increased with the concentrations of HA increased from 50 ppm to 500 ppm. Apparently, the HA -goethite complex presented the better photoinductive activity than goethite. It has been reported that in sunlit surface waters containing natural organic matter, photochemical reactions can result in the rapid formation of both Fe(II) through LMCT reactions of Fe(III)-organic complexes and H_2O_2 mainly through the reduction of oxygen by photo-excited organic substances [19, 30]. The related main reactions occurring in systems containing HA and Fe(III) are as follows:

$$FeOOH + HA \rightarrow Fe(\mathrm{III}) - HA \quad (7)$$

$$HA + hv \rightarrow HA^* \quad (8)$$

$$HA^* + O_2 \rightarrow Products + O_2^{\bullet-} / HO_2^{\bullet} \quad (9)$$

$$O_2^{\bullet-} / HO_2^{\bullet} \rightarrow H_2O_2 \quad (10)$$

$$Fe(\mathrm{III}) - HA + hv \rightarrow HA^{\bullet+} + Fe(\mathrm{II}) \quad (11)$$

$$Fe(\mathrm{II}) + O_2 \rightarrow Fe(\mathrm{III}) + O_2^{\bullet-} / HO_2^{\bullet} \quad (12)$$

$$Fe(\text{II}) + H_2O_2 \rightarrow Fe(\text{III}) + {}^{\bullet}OH + OH^{-} \quad (13)$$

$$TYL / SMT + {}^{\bullet}OH \rightarrow \text{Products} \quad (14)$$

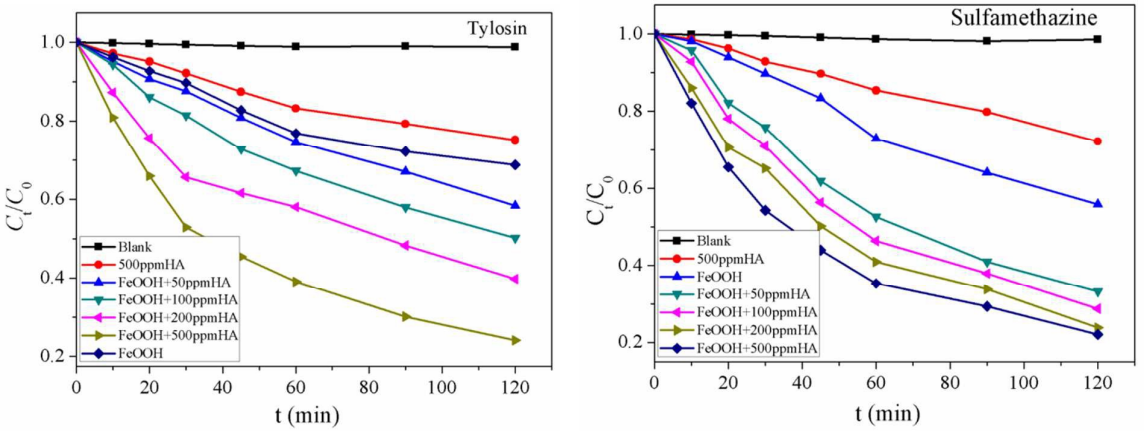

Fig. 8 Photodegradation of TYL and SMT by goethite, HA and HA -goethite complexes (the pH for TYL and SMT were 3.5; temperature = 25 ^{0}C; I = 0.01 M KNO_3)

Therefore, the concentration of Fe(II) and H_2O_2 photoformed in the solutions during TYL and SMT photodegradation was measured (Fig. 9). As shown in Fig.9, the concentrations of Fe(II) and H_2O_2 were increased with the concentrations of HA increased from 50 ppm to 500 ppm, indicating that more oxidants (e.g. • OH, formed by reaction of Fe(II) with H_2O_2) could be generated in the presence of both Fe(III) and HA, thus accelerating the photodegradation of TYL and SMT [31].

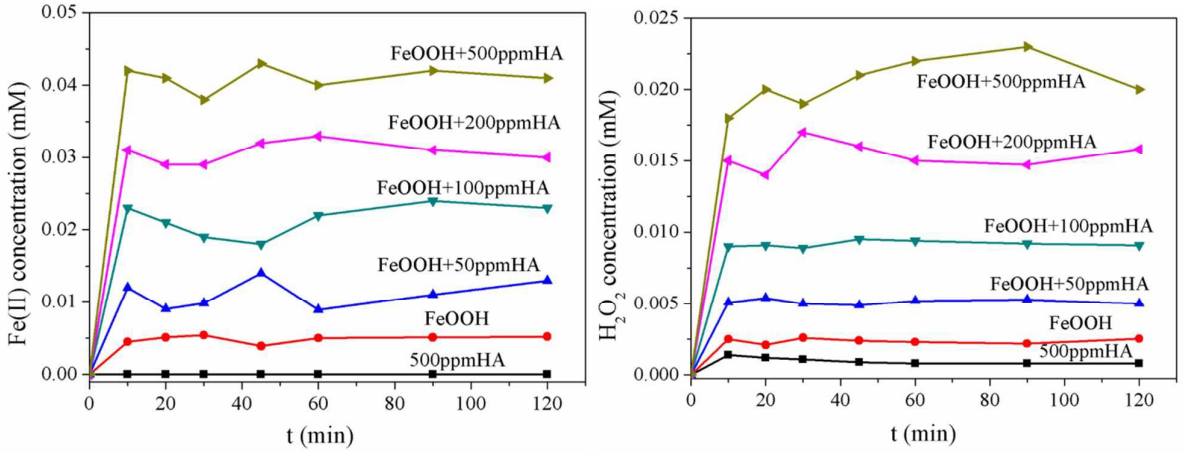

Fig. 9 The corresponded concentrations of H_2O_2 and Fe(II) photoformed in different concentrations of HA

On the basis of above discussions, a possible reaction mechanism in the presence of Fe(III)–HA complex was proposed in Fig. 10. When HA and goethite coexist in solution, HA might react with iron species followed by the formation of iron-HA complexes, and photochemical reactions of these

complexes take place by electron transfer from HA to the Fe(III) which could produce Fe(II) and consume HA. Then the reaction of the free humic radical with O_2 leads to $O_2^{\bullet-}/HO_2^{\bullet}$ formation, and H_2O_2 is the product of $O_2^{\bullet-}/HO_2^{\bullet}$ dismutation. Ultimately, the simultaneous and rapid photoformation of Fe(II) and H_2O_2 in the irradiated Fe(III)-HA system leads to •OH formation. However, there are numerous concurrent processes in the systems, including the competing reactions of free HA radical ($HA^{\bullet+}$) with O_2 and Fe(III) species, and the •OH quenched by both TYL/SMT and HA. The net result was an iron redox cycle in which HA as well as oxygen were consumed, ROS were generated and reacted, and the degradation of TYL/SMT was accelerated[19, 31].

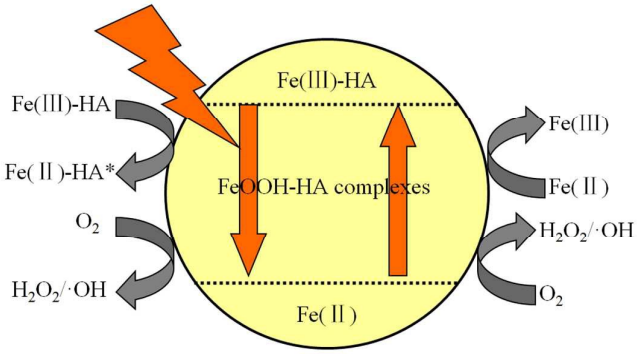

Fig. 10 The iron cycling and main reactions in Fe(III)-HA complexes systems

4. Conclusion

Our results presented an investigation of HA and goethite interaction and their effects on TYL and SMT sorption and photodegradation, which was significant in the natural environment as HA abundantly coexist in surface with iron and antibiotics. The characteristic results showed that goethite binding of HA through ligand exchange and there were the structure changes of goethite after complex with HA. The sorption and photodegradation of TYL/SMT in soils was obviously influenced by goethite and HA. The present study showed that HA -goethite complexes has a high sorption capacity and sorption rate for sorption of TYL and SMT, probably due to the heterogeneous surface of HA. The photodegradation of TYL and SMT by HA -goethite complexes were increased with the concentrations of HA increased. An iron redox cycle coupled should be a common phenomenon in the system, since both Fe(III) and HA were ubiquitous in the natural environment. This study is

helpful in understanding the potential of toxic organic pollutants migration and transformation in natural environmental.

Acknowledgements

The study was financially supported by the China National Science Fund Program (Nos. 41503095, 41173104), the Natural Science Foundation of Universities of Anhui Province (KJ2015A016), the PhD Fund of Anhui University of Science and Technology (ZY540) and the Key Science Foundation for Young Teachers of Anhui University of Science and Technology (QN201507).

References

1. Z. Pei, S. Yang, L. Li, C. Li, S. Zhang, X.-q. Shan, B. Wen and B. Guo, *Environmental Pollution*, 2014, **184**, 579-585.
2. R. Zhang, J. Tang, J. Li, Z. Cheng, C. Chaemfa, D. Liu, Q. Zheng, M. Song, C. Luo and G. Zhang, *Science of the Total Environment*, 2013, **450**, 197-204.
3. X. Guo, C. Yang, Y. Wu and Z. Dang, *Environ Sci Pollut Res*, 2014, **21**, 2572-2580.
4. D. Mutavdžić Pavlović, L. Ćurković, D. Blažek and J. Župan, *Science of the Total Environment*, 2014, **497–498**, 543-552.
5. L. Zhao, Z.-r. Lin and Y.-h. Dong, *Environ Sci Pollut Res*, 2014, **21**, 2688-2696.
6. Q. Zhang, C. Yang, W. Huang, Z. Dang and X. Shu, *Chemosphere*, 2013, **93**, 2180-2186.
7. X. Guo, C. Yang, Z. Dang, Q. Zhang, Y. Li and Q. Meng, *Chemical Engineering Journal*, 2013, **223**, 59-67.
8. V. Leone, P. Iovino, S. Salvestrini and S. Capasso, *Chemosphere*, 2014, **95**, 75-80.
9. Y. Zhao, X. Gu, S. Gao, J. Geng and X. Wang, *Geoderma*, 2012, **183**, 12-18.
10. Y. Zhao, F. Tong, X. Gu, C. Gu, X. Wang and Y. Zhang, *Science of the Total Environment*, 2014, **470**, 19-25.
11. H. Liu, T. Chen and R. L. Frost, *Chemosphere*, 2014, **103**, 1-11.
12. M. Kersten, D. Tunega, I. Georgieva, N. Vlasova and R. Branscheid, *Environmental Science & Technology*, 2014, **48**, 11803-11810.
13. J. Gao and J. A. Pedersen, *Journal of Environmental Quality*, 2010, **39**, 228-235.
14. S. K. Han, T.-M. Hwang, Y. Yoon and J.-W. Kang, *Chemosphere*, 2011, **84**, 1095-1101.
15. H. Wu, X. Dou, D. Deng, Y. Guan, L. Zhang and G. He, *Environmental Technology*, 2012, **33**, 1545-1552.
16. M. Brigante, G. Zanini and M. Avena, *Journal of Hazardous Materials*, 2010, **184**, 241-247.
17. K. Yang and B. Xing, *Environmental Science & Technology*, 2009, **43**, 1845-1851.
18. L. Ji, W. Chen, L. Duan and D. Zhu, *Environmental Science & Technology*, 2009, **43**, 2322-2327.
19. X. Ou, S. Chen, X. Quan and H. Zhao, *Chemosphere*, 2008, **72**, 925-931.
20. S. Zhang, W. Xu, M. Zeng, J. Li, J. Li, J. Xu and X. Wang, *Journal of Materials Chemistry A*, 2013, **1**, 11691-11697.
21. L. Peng, P. Qin, M. Lei, Q. Zeng, H. Song, J. Yang, J. Shao, B. Liao and J. Gu, *Journal of Hazardous Materials*, 2012, **209**, 193-198.
22. S. Zhang, J. Li, X. Wang, Y. Huang, M. Zeng and J. Xu, *Journal of Materials Chemistry A*, 2015, **3**, 10119-10126.

23. F. Fathollahi, M. Javanbakht, H. Omidvar and M. Ghaemi, *Journal of Alloys and Compounds*, 2015, **643**, 40-48.
24. H. Wang, J. Zhu, Q.-L. Fu, J.-W. Xiong, C. Hong, H.-Q. Hu and A. Violante, *Pedosphere*, 2015, **25**, 405-414.
25. H. Peng, N. Liang, H. Li, F. Chen, D. Zhang, B. Pan and B. Xing, *Environmental pollution (Barking, Essex : 1987)*, 2015, **204**, 191-198.
26. X. Guo, J. Ge, C. Yang, R. Wu, Z. Dang and S. Liu, *RSC Adv.*, 2015, **5**, 58865-58872.
27. F. Lian, B. Sun, X. Chen, L. Zhu, Z. Liu and B. Xing, *Environmental pollution (Barking, Essex : 1987)*, 2015, **204**, 306-312.
28. S. Zhang, J. Li, M. Zeng, G. Zhao, J. Xu, W. Hu and X. Wang, *ACS Applied Materials & Interfaces*, 2013, **5**, 12735-12743.
29. Y. Li, C. Yang, X. Guo, Z. Dang, X. Li and Q. Zhang, *Chemosphere*, 2015, **119**, 171-176.
30. S. Zhang, M. Zeng, J. Li, J. Li, J. Xu and X. Wang, *Journal of Materials Chemistry A*, 2014, **2**, 4391-4397.
31. X. Ou, X. Quan, S. Chen, H. Zhao and Y. Zhang, *Journal of Agricultural and Food Chemistry*, 2007, **55**, 8650-8656.